



COB-2021-0558

Macroscopic mechanical behavior of polymeric foams via finite element analysis of a representative volume element

Eliardo Gabriel Rezende Martins

Heloísa Zanardi

Ricardo Afonso Angélico

University of São Paulo, São Carlos School of Engineering, Department of Aeronautics Engineering

eliardo.martins@usp.br, heloisa.zanardi@usp.br, raa@sc.usp.br

Abstract. *Polymeric foam materials are used in engineering applications that require low-weight materials with low thermal conductivity, capability to withstand large deformations or impact energy absorption. The macroscopic foam mechanical behavior is a consequence of material microstructure and its intrinsic deformation mechanisms. Numerical tools are useful to predict the macroscopic mechanical behavior of foam materials from their microstructure. In particular, finite element simulations can be performed on Representative Volume Element (RVE) to estimate its effective mechanical properties. In this context, the present article aims to predict the macroscopic mechanical behavior of polymeric foams via finite element analysis of random RVEs. The authors developed a computational tool in Python with three modules: (i) RVE creation; (ii) creation of finite element model; and (iii) identification of macroscopic mechanical behavior. First, a Voronoi tessellation algorithm developed in Python enables creating the artificial foam microstructure. The RVE created is periodic concerning the geometry and the mesh, and it is imported into Abaqus finite element package for analysis. Second, the tool identifies the opposite correspondent nodes and applies a periodic boundary condition. Macroscopic strain components can be applied via two reference points. For each foam closed-cell, a self-contact interaction with hard-contact and no friction behavior is used. And lastly, the macroscopic stress and strain tensor components are obtained via the RVE domain integration. The tool is applied to predict the macroscopic behavior of a 60 kg/m³ polymeric foam for several strain states and with different microstructure characteristics. The simulations were performed with a elastic and an elasto-plastic material model. The RVE were analysed under controlled macrostrain history, which is applied via the reference points. The results are compared with analytical predictions. The RVE analysis enabled to simulate the linear elastic, plateau and densification stages of the foam under compression.*

Keywords: *mechanical behavior, polymeric foams, representative volume element, effective properties, finite element method, periodic boundary conditions.*

1. INTRODUCTION

Cellular materials are present in stiff and low-weight natural materials, e.g., wood, bones, coral, and sponge (Gibson and Ashby, 1982). In engineering, foam-like materials are adopted where low thermal conductivity, low weight, and high energy absorption capability are required (Avallée et al., 2001; Wu et al., 1999). The macroscopic mechanical behavior of foams is directly associated with their microstructure and intrinsic deformation mechanisms (Gibson and Ashby, 1982). Under uniaxial compression, the foam presents three typical phases: linear, plateau, and densification (Rusch, 1969). The microstructure deformation mechanisms of each phase enable to explain the foam mechanical macroscopic behavior, as reported by the literature (Viot et al., 2005; Mills and Zhu, 1999; Maitiet et al., 1984).

Numerical tools are helpful to predict the macroscopic mechanical behavior of foam materials from their microstructure (Ozturk and Anlas, 2011). In particular, finite element simulations can be performed on Representative Volume Element (RVE) to predict the macroscopic behavior of the material (Sun and Vaidya, 1996). The finite element analysis of foam-like structures contributes to understanding deformation mechanisms, and consequently, the macroscopic response of the material when submitted to loading. Also, with the advances in manufacturing techniques, they help investigate how the microstructure parameters influence macroscopic properties (Royet et al., 2016). The finite element analysis has been used mainly to predict effective macroscopic properties of engineering materials (Xia et al., 2003; Kariet et al., 2007; Xu and Xu, 2008). Tang et al. (2014) investigate the influence of foam cell irregularities on macroscopic behavior, using 2D and 3D models created using Voronoi tessellation.

In this context, the present article aims to predict the macroscopic behavior of a PVC polymeric foam using finite element simulations of a random RVE. The article describes the procedure involved in geometry creation, application of the periodic boundary conditions and definition of self-contact in the foam cells. The created RVE models were analyzed, and their macroscopic behavior is reported for uniaxial compression loading. The finite element model developed in the

present article considers a random bidimensional microstructure based on bidimensional Voronoi tessellation. Despite different types of numerical models, few explore the simulation of the densification process using a contact model. The present article assembles the contribution of several authors in the analysis of polymeric foam.

2. METHODOLOGY

2.1 Closed-cell foam RVE creation

The generation of a random RVE was divided in four parts: (i) generation of a periodic geometry for the microstructure (PGC); (ii) generation of a periodic mesh (PMC); (iii) prescription of periodic boundary conditions for the boundary elements (PBC); and (iv) generation of self-contact conditions under compression (SCC). These modules were developed to operate in conjunction with Abaqus[™] finite element software. Using the *Abaqus Scripting Interface Systèmes* (2014), the user can develop routines in Python to enhance the software functionalities.

2.1.1 Periodic geometry and mesh creation (PGC / PMC)

The periodic geometry creation is based on the 2D Voronoi tessellation, which can be created based on several parameters (Torquato, S. and Haslach HW, Jr., 2002). Herein, the microstructure is controlled by five parameters: (i) number and location of Voronoi sites; (ii) perturbation factor; (iii) offset method; (iv) microstructure wall thickness; and (v) internal corner radius. The Voronoi tessellation is determined by the initial site distribution, then each site distribution generates a specific pattern of cell areas. In the present work, sites are allocated assuming a regular microstructure and posteriorly, the Voronoi sites location are perturbed by a random value. The initial regular microstructure pattern and its configuration after the perturbation can be seen in Fig. 1.

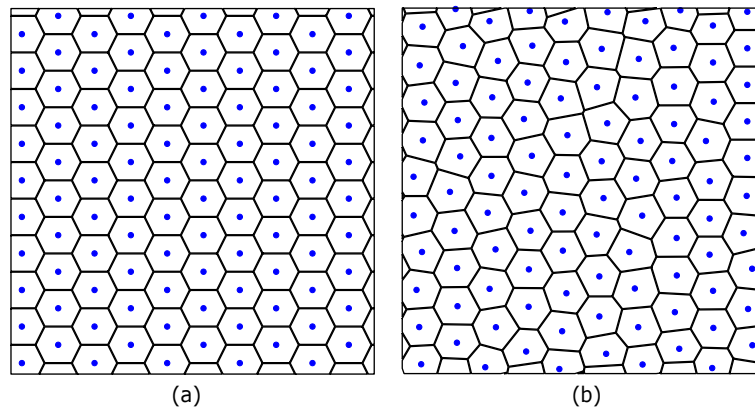


Figure 1. Voronoi tessellation sites distribution: (a) initial configuration; (b) after sites disturbance.

Aiming to obtain a periodic cellular microstructure, the algorithm replicates the initial Voronoi sites to the eight adjacent regions (Fig. 2). This procedure assures the central region is periodic in every direction. After having a periodic microstructure based on the Voronoi tessellation, the foams cells geometries are created using the Python library *Shapely* (Gillies *et al.*, 2007–) that can carry out geometrical operations in polygons. The foam cells can be constructed using four different offset methods, which are illustrated in (Fig. 3). The user can choose which is more representative for the analyzed case. In the present article, the offset is created considering a specified value for wall thickness and corner radius (Fig. 3c). Thus, it has been created a data structure in Python to enclose all the polygons after the offset operations.

Seeking to separate the periodic domain, which is the central part that had already been created in the whole Voronoi tessellation, the intersection algorithms of *Shapely* (Gillies *et al.*, 2007–) have been used. For that, firstly, the polygons were classified into internal, external, and boundary polygons. And, iterating over the list of boundary polygons, it has been possible to intersect all the boundary polygons with the domain. As a result, all the polygons are periodic and self-contained in the domain of interest (Fig. 4).

GMsh was used to generate and mesh the model since Abaqus[™], despite being a finite element package with several functionalities, does not offer resources that allow the creation of periodic meshes. GMsh has a Python API (Application Programming Interface) that allows a relatively simple connection with Abaqus[™]. GMsh is an open-source 3D finite element mesh generator with two CAD engine kernels ("Built-in" and "OpenCascade") that enables to create and mesh complex geometries with several types of elements (Geuzaine and Remacle, 2009). The "Built-in" kernel has a bottom-up approach, while the second one offers a constructive solid geometry approach. Therefore, considering the desired models, "OpenCascade (OCC)" kernel together with *Shapely* library were adopted to create the geometries with a periodic mesh.

The mesh is controlled by two parameters: (i) mesh size factor, and (ii) element order. The mesh size factor determines the overall RVE element size. In the present work, the maximum mesh size factor may be the same order of the wall

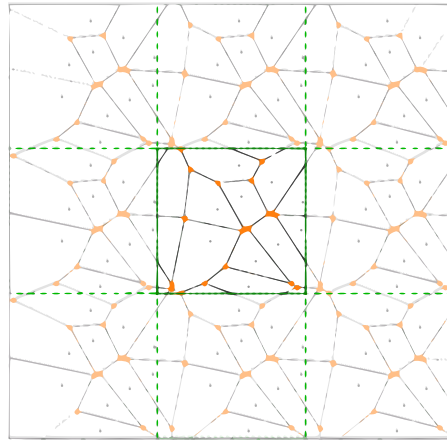


Figure 2. Creation of a RVE with periodic geometry.

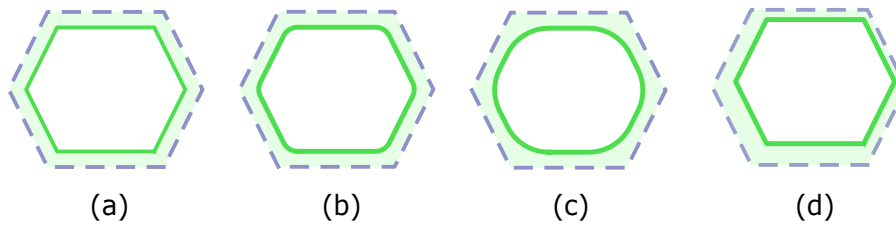


Figure 3. Alternatives for creation of the foam cells: (a) offset by specified value with flat corner; (b) offset by specified value with round corner; (c) offset by specified value with specified corner radius; and (d) offset by scale.

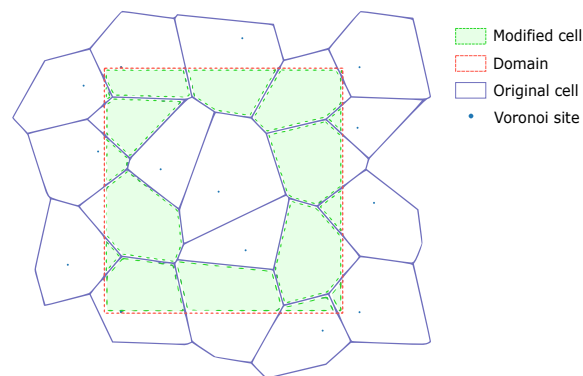


Figure 4. Creation of the RVE domain.

thickness. The element order parameter describes which element is generated and, consequently, which kind of element will be used in Abaqus, and it can assume the values of 1 (linear) or 2 (quadratic). Only triangular elements were available at the current version of in-house software.

2.1.2 Periodic boundary condition (PBC)

In this work, in order to accurately simulate a finite element RVE model for a cellular solid, it is necessary to apply periodic boundary conditions (PBC). The PBCs assure the displacement and traction continuities between neighboring RVEs (Xu and Xu, 2008). The first step in the application of the PBCs is the establishment of a correlation between the nodes belonging to opposite RVE entities (edges and vertices). The previous creation of a periodic mesh facilitates this process, reducing it to a simple identification of node labels. Once the node pairs are identified, a set of equations is applied. They relate the displacements along directions 1 and 2 (u and v , respectively) of the nodes with the macroscopic

applied strains $\bar{\varepsilon}_{xx}$, $\bar{\varepsilon}_{yy}$, and $\bar{\varepsilon}_{xy}$ as proposed by Ye and Wang (2017) and shown below:

$$\begin{aligned} u_{BC} - u_{AD} &= \ell_x \bar{\varepsilon}_{xx} \\ v_{BC} - v_{AD} &= \ell_x \bar{\varepsilon}_{xy} \\ u_{CD} - u_{AB} &= \ell_y \bar{\varepsilon}_{xy} \\ v_{CD} - v_{AB} &= \ell_y \bar{\varepsilon}_{yy} \end{aligned} \quad (1)$$

and for its vertex as:

$$\begin{aligned} u_C - u_A &= \ell_x \bar{\varepsilon}_{xx} + \ell_y \bar{\varepsilon}_{xy} \\ v_C - v_A &= \ell_y \bar{\varepsilon}_{yy} + \ell_x \bar{\varepsilon}_{xy} \\ u_B - u_D &= \ell_x \bar{\varepsilon}_{xx} - \ell_y \bar{\varepsilon}_{xy} \\ v_B - v_D &= -\ell_y \bar{\varepsilon}_{yy} + \ell_x \bar{\varepsilon}_{xy} \end{aligned} \quad (2)$$

where ℓ_x is the RVE width and ℓ_y its height. For the considered model, the RVE vertices are located in regions without material. Therefore, Eq. (2) will not be applied. For displacement-based finite element analysis, Equations (1) to (2) suffice to assure the traction continuity too, as demonstrated by Xia *et al.* (2003).

2.2 Finite element RVE model

The RVE was modeled considering a PVC Young modulus $E = 3$ GPa and Poisson ratio $\nu = 0.3$ (Colloca *et al.*, 2012). The cells on RVE [HZ: The RVE's cells] are almost irregular hexagons. The RVE was discretized using linear triangular elements for plane strain analysis (Fig. 5). The RVE is submitted to uniaxial compressions on horizontal direction.

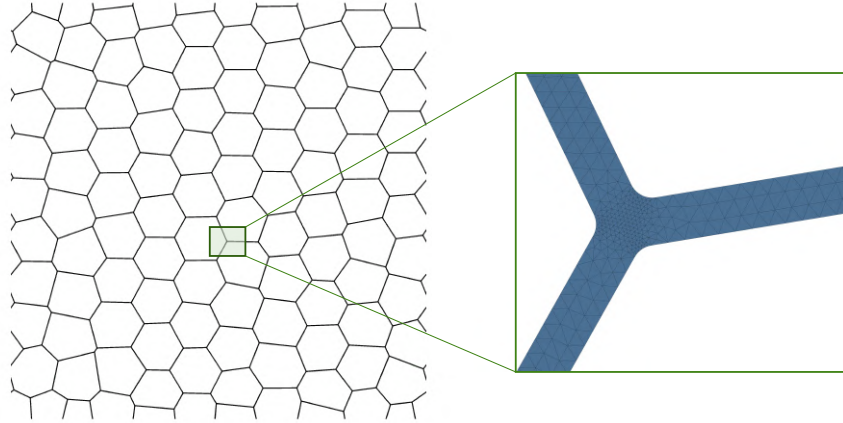


Figure 5. Mesh detail on wall and corner regions.

The foam densification process happens throughout the compression, after the buckling of the cell walls, which is succeeded by the contact between its internal surfaces. This phenomenon changes the macroscopic mechanical behavior of the foam. Therefore, the contact model ensures the non-penetration between cell walls. Thereby, the contact model was modeled as a self-contact. The model adopted herein considers a hard contact for the normal behavior and a frictionless contact for the tangential behavior.

2.3 Determination of macroscopic stress and strain components

The macroscopic strains are applied on the RVE, and the macrostress can be obtained integrating stress components over the RVE volume. According to the homogenization method (Nemat-Nasser and Hori, 2013; Smit *et al.*, 1998; Sun and Vaidya, 1996), the macroscopic stress and strain tensors can be computed as:

$$\bar{\boldsymbol{\sigma}} = \frac{1}{V_{RVE}} \int_{V_{RVE}} \boldsymbol{\sigma}(\mathbf{x}) dV \quad (3)$$

$$\bar{\boldsymbol{\varepsilon}} = \frac{1}{V_{RVE}} \int_{V_{RVE}} \boldsymbol{\varepsilon}(\mathbf{x}) dV \quad (4)$$

where V_{RVE} is the RVE volume. The integration was performed using the stress and strain components evaluated at each element integration point. In particular, from the macroscopic components obtained using Eq. (3) and (4), the macroscopic constitutive tensor can be identified submitting the RVE to different loading cases.

3. RESULTS

The foam deformed configuration at several loading levels can be seen in Fig. 6 for the RVE 1. At initial loading states, the foam walls start to present a local buckling (Fig. 6(b)). This behavior continues until neighbor walls start the contact between neighbor walls (Fig. 6(e)). Snapshots of [HZ: the] RVE for different loading levels showed the formation of bands of compression, which was also observed experimentally (Caliri Júnior *et al.*, 2012), and [HZ: they] are a consequence of the RVE randomness. The periodic boundary condition was correctly implemented (Fig. 7), but the contact between periodic cells could not be established. The self-contact condition cannot be applied for some cells close to the RVE borders, as shown on the green rectangle (Fig. 7), and interpenetration between solid regions was observed. This phenomenon is difficult to be avoided, and it only occurs in small amounts of the cells, which does not compromise the RVE macroscopic behavior.

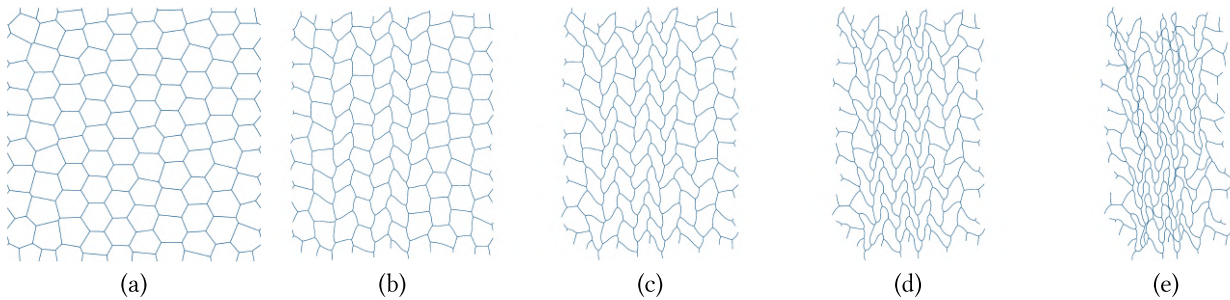


Figure 6. RVE at different macrostrain levels for a uniaxial compression at x-direction: (a) $\bar{\varepsilon} = 0.0$ (initial configuration), (b) $\bar{\varepsilon} = -0.125$, (c) $\bar{\varepsilon} = -0.250$, (d) $\bar{\varepsilon} = -0.375$, (e) $\bar{\varepsilon} = -0.500$.

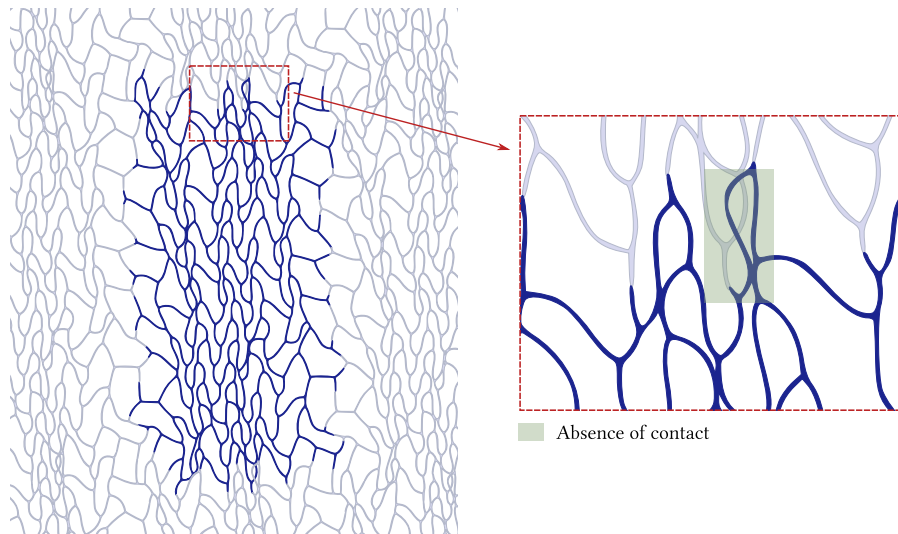


Figure 7. Region of RVE that does not verify the contact condition.

The macroscopic stress vs. strain for the RVE can be seen in Fig. 8. The blue line corresponds to RVE-1, and the points (a) up to (e) correspond to the pictures shown in Fig. 6. The gray lines on the background are the response for RVE-2 up to RVE-5. From the macroscopic response, the effective Young modulus of 0.5134 ± 0.0049 MPa was obtained. The two-dimensional random RVE analyzed herein does not consider the stiffness contribution from outside cell walls with normal out-of-plane. This behavior [HZ: is corroborated by / corroborates] corroborates for the lower Young modulus. Furthermore, it can explain the foam softening after reaching the maximum stress level. The foam stiffness tends to increase as the contact between the walls increases, however, problems of convergence prevented from proceeding with higher deformation levels.

In order to validate the results obtained from the present work with the theoretical results, the relationship between the cellular solid elastic modulus from this work and the original solid elastic modulus for hexagonal honeycomb materials under uniaxial loading from (Gibson and Ashby, 1982) was analyzed. The theoretical Young modulus for a regular hexagonal material is given by:

$$E^* = \frac{\sqrt{3}}{8} \left(\frac{\rho^*}{\rho_S} \right)^3 \frac{\cos(\theta)}{[h/\ell + \sin(\theta)] \sin^2(\theta)} \quad (5)$$

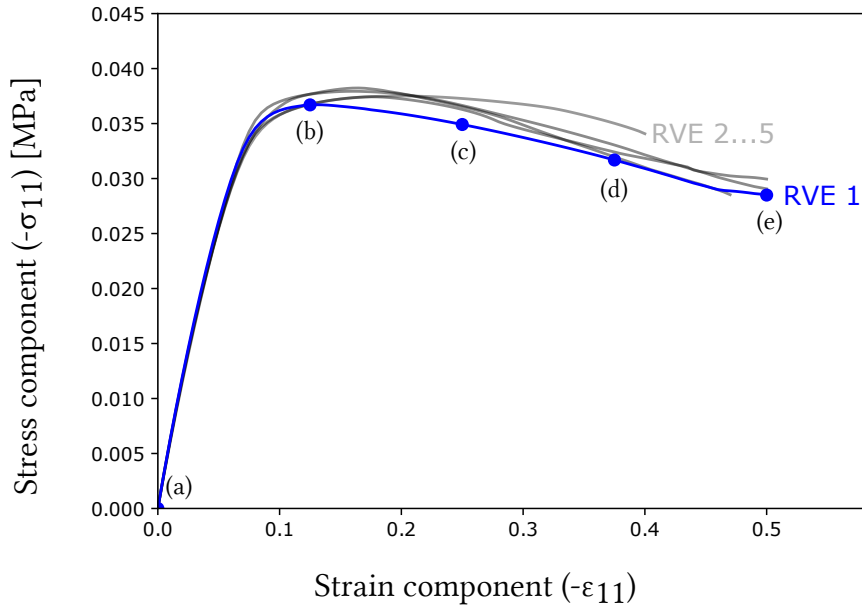


Figure 8. Stress vs. strain response for the RVEs analyzed.

where ρ^*/ρ_S is the apparent density, ℓ is the length of the hexagonal cell edge, h is the height of the hexagonal cell, θ the angle between the x-axis and the tilted edge of the hexagonal cell and E^* is the elastic modulus in-plane direction. The comparison between the predicted Young modulus and Gibson model is shown in Fig. 9.

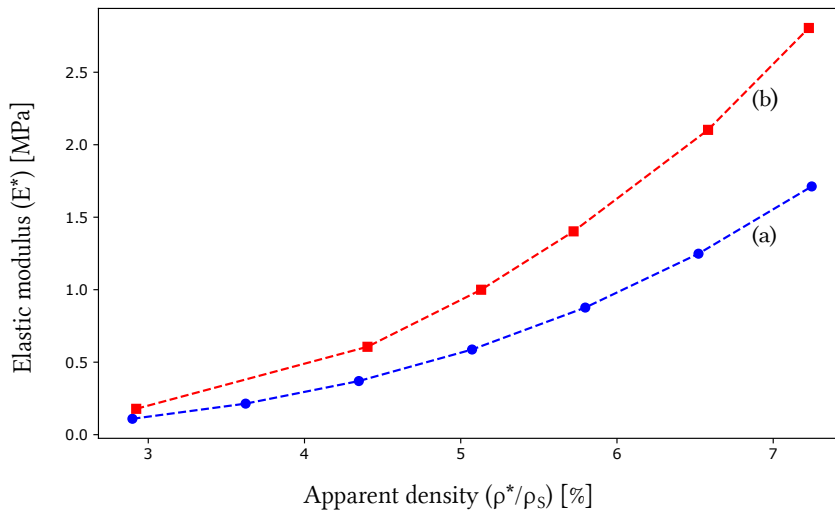


Figure 9. Elastic modulus vs. apparent density: (a) theoretical approach (Gibson and Ashby, 1982); and (b) numerical approach.

4. CONCLUSIONS

The present article was dedicated to the development of RVE to represent the macroscopic behavior of PVC foams under uniaxial compression. The predicted Young modulus is compared with literature data. Snapshots of RVE for different loading levels show the formation of bands of compression, and enable to visualize the microstructure deformation mechanisms. The fact that out-of-plane stiffness is not considered contributes to the creation of mechanisms that leads to the material softening. Convergence problems prevented from analyzing the microstructure at higher deformation levels. The following developments concern the implementation of 3D models and evaluating RVE behavior at several stress states, aiming to obtain a correspondence between macroscopic material behavior and microstructure parameters.

5. ACKNOWLEDGEMENTS

The authors would like to thank the National Council for Scientific and Technological Development (CNPq Proc. 141041/2019-6) and *Programa Unificado de Bolsas de Estudos para Estudantes de Graduação* (PUB, Proc. 2791/2018) for the financial support on this project.

6. REFERENCES

- Caliri Júnior, M., Soares, G., Angélico, R., Canto, R. and Tita, V., 2012. “Study of an anisotropic polymeric cellular material under compression loading”. *Materials Research*, Vol. 15, No. 3. ISSN 15161439. doi: 10.1590/S1516-14392012005000034.
- Colloca, M., Dorogokupets, G., Gupta, N. and Porfiri, M., 2012. “Mechanical properties and failure mechanisms of closed-cell PVC foams”. *International Journal of Crashworthiness*, Vol. 17, No. 3, pp. 327–336. ISSN 13588265. doi:10.1080/13588265.2012.661637.
- Geuzaine, C. and Remacle, J.F., 2009. “Gmsh: A 3-d finite element mesh generator with built-in pre-and post-processing facilities”. *International journal for numerical methods in engineering*, Vol. 79, No. 11, pp. 1309–1331.
- Gibson, I. and Ashby, M.F., 1982. “The mechanics of three-dimensional cellular materials”. *Proceedings of the royal society of London. A. Mathematical and physical sciences*, Vol. 382, No. 1782, pp. 43–59.
- Gillies, S. *et al.*, 2007–. “Shapely: manipulation and analysis of geometric objects”. URL <https://github.com/Toblerity/Shapely>.
- Nemat-Nasser, S. and Hori, M., 2013. *Micromechanics: overall properties of heterogeneous materials*. Elsevier.
- Smit, R.J., Brekelmans, W.A. and Meijer, H.E., 1998. “Prediction of the mechanical behavior of nonlinear heterogeneous systems by multi-level finite element modeling”. *Computer Methods in Applied Mechanics and Engineering*, Vol. 155, No. 1-2, pp. 181–192. ISSN 00457825. doi:10.1016/S0045-7825(97)00139-4.
- Sun, C.T. and Vaidya, R.S., 1996. “Prediction of composite properties from a representative volume element”. *Composites Science and Technology*, Vol. 56, No. 2, pp. 171–179. ISSN 02663538. doi:10.1016/0266-3538(95)00141-7.
- Systèmes, D., 2014. “Abaqus 6.14 online documentation”. *Abaqus Scripting Reference Guide*.
- Torquato, S. and Haslach HW, Jr., 2002. “Random Heterogeneous Materials: Microstructure and Macroscopic Properties”. *Applied Mechanics Reviews*, Vol. 55, No. 4, pp. B62–B63. ISSN 0003-6900. doi:10.1115/1.1483342. URL <https://doi.org/10.1115/1.1483342>.
- Xia, Z., Zhang, Y. and Ellyin, F., 2003. “A unified periodical boundary conditions for representative volume elements of composites and applications”. *International journal of solids and structures*, Vol. 40, No. 8, pp. 1907–1921.
- Xu, K. and Xu, X., 2008. “Finite element analysis of mechanical properties of 3d five-directional braided composites”. *Materials Science and Engineering: A*, Vol. 487, No. 1-2, pp. 499–509.
- Ye, F. and Wang, H., 2017. “A simple python code for computing effective properties of 2d and 3d representative volume element under periodic boundary conditions”. *arXiv preprint arXiv:1703.03930*.

7. RESPONSIBILITY NOTICE

The authors are solely responsible for the printed material included in this paper.